Published in final edited form as:
Mov Disord. 2011 September ; 26(11): 2032–2038. doi:10.1002/mds.23778.

A Within-Subject Comparison of 6-[18F]Fluoro-m-tyrosine and 6-[18F]Fluoro-L-dopa in Parkinson's Disease

Catherine L. Gallagher, MD[1,2,*], **Bradley T. Christian, PhD**[3,4], **James E. Holden, PhD**[3], **Onofre T. Dejesus, PhD**[3], **Robert J. Nickles, PhD**[3], **Laura Buyan-Dent, MD, PhD**[2], **Barbara B. Bendlin, PhD**[5,6], **Sandra J. Harding, MS**[5,6], **Charles K. Stone, MD**[6], **Barb Mueller, BS**[4], and **Sterling C. Johnson, PhD**[5,6]

[1]William S. Middleton Veterans Hospital, Madison, Wisconsin, USA

[2]Department of Neurology, University of Wisconsin School of Medicine and Public Health, Madison, Wisconsin, USA

[3]University of Wisconsin, Department of Medical Physics, Madison, Wisconsin, USA

[4]Waisman Laboratory for Brain Imaging and Behavior, Madison, Wisconsin, USA

[5]William S. Middleton Veterans Hospital G.R.E.C.C., Madison, Wisconsin, USA

[6]Department of Medicine, University of Wisconsin School of Medicine and Public Health, Madison, Wisconsin, USA

Abstract

Progression of Parkinson's disease symptoms is imperfectly correlated with positron emission tomography biomarkers for dopamine biosynthetic pathways. The radiopharmaceutical 6-[^{18}F]fluoro-m-tyrosine is not a substrate for catechol-O-methyltransferase and therefore has a more favorable uptake-to-background ratio than 6-[^{18}F]fluoro-L-dopa. The objective of this study was to evaluate 6-[^{18}F]fluoro-m-tyrosine relative to 6-[^{18}F]fluoro-L-dopa with partial catechol-*O*-methyltransferase inhibition as a biomarker for clinical status in Parkinson's disease. Twelve patients with early-stage Parkinson's disease, off medication, underwent Unified Parkinson Disease Rating Scale scoring, brain magnetic resonance imaging, and 3-dimensional dynamic positron emission tomography using equivalent doses of 6-[^{18}F]fluoro-m-tyrosine and 6-[^{18}F]fluoro-L-dopa with tolcapone, a catechol-*O*-methyltransferase inhibitor. Images were realigned within subject, after which the tissue-derived uptake rate constant was generated for volumes of interest encompassing the caudate nucleus, putamen, and subregions of the putamen. We computed both bivariate (Pearson) and partial (covariate of age) correlations between clinical subscores and tissue-derived uptake rate constant. Tissue-derived uptake rate constant values were correlated between the radiopharmaceuticals ($r = 0.8$). Motor subscores were inversely correlated with the contralateral putamen 6-[^{18}F]fluoro-m-tyrosine tissue-derived uptake rate constant ($|r| > 0.72$, $P < .005$) but not significantly with the 6-[^{18}F]fluoro-L-dopa tissue- derived uptake rate constant. The uptake rate constants for both radiopharmaceuticals were also inversely correlated with activities of daily living subscores, but the magnitude of correlation coefficients was greater for 6-[^{18}F]fluoro-m-tyrosine. In this design, 6-[^{18}F]fluoro-m-tyrosine uptake better reflected clinical status than did 6-[^{18}F]fluoro-L-dopa uptake. We attribute this finding to 6-[^{18}F]fluoro-m-

[*]**Correspondence to:** Dr. Catherine L. Gallagher, William S. Middleton V.A. and University of Wisconsin Department of Neurology, 2500 Overlook Terrace Dr., Madison, WI, 53705, USA; gallagher@neurology.wisc.edu.

Relevant conflicts of interest/financial disclosures: Nothing to report.
Full financial disclosures and author roles may be found in the online version of this article.

tyrosine's higher affinity for the target, L-aromatic amino acid decarboxylase, and the absence of other major determinants of the uptake rate constant. These results also imply that L-aromatic amino acid decarboxylase activity is a major determinant of clinical status.

Keywords

positron emission tomography; Parkinson's disease/radionuclide imaging; dopamine/metabolism

Specific uptake of radiopharmaceutical agents such as [^{18}F]fluoro-L-dopa (FDOPA) that target central dopamine biosynthetic pathways have been used as surrogate outcome measures in Parkinson's disease (PD) clinical trials.[1] However, longitudinal changes in striatal uptake of FDOPA, imaged using positron emission tomography (PET), do not correlate optimally with clinical measures of disease progression.[2,3] Furthermore, kinetic modeling of FDOPA uptake is complicated by variability in its rate of loss[4] and by its COMT metabolite, 3-*O*-methyl-FDOPA (3OMD), which crosses the blood–brain barrier to reduce signal to background.[5] Another radiotracer that targets L-aromatic amino acid decarboxylase (AADC) 6-[^{18}F]fluoro-m-tyrosine (FMT) offers advantages over FDOPA in that it has higher affinity for the target and is not a substrate for catechol-*O*-methyltransferase (COMT).[6] FMT PET has been used widely in nonhuman primate models of PD but infrequently in human studies. In the past, dosimetry data from studies in which carbidopa pretreatment was not used have limited the dose of FMT to 2.5 mCi to keep bladder wall exposure under 5 rads.[7] Although some previous studies have used 5 mCi of FMT in humans,[8,9] others have used 2.5 mCi.[10,11] The primary goal of this study was to validate the performance of FMT as a correlate of clinical symptoms in PD. A secondary goal was to investigate comparative bladder wall radiation dosimetry for FDOPA and FMT in this study population.

Patients and Methods

Twelve subjects (mean age, 61 years; SD, 9.3 years; 10 men) with Hoehn and Yahr stages 1–3 idiopathic Parkinson's disease (PD) by UK Brain Bank criteria,[12] normal liver function, and the absence of other major disease were recruited from local movement disorders clinics. Of these subjects, 5 were taking monoamine oxidase inhibitors (MAOIs), 7 were taking dopamine agonists (pramipexole or ropinerole), and 3 were taking carbidopa/levodopa (750–1200 mg of levodopa daily). Procedures included brain FDOPA and FMT PET imaging, magnetic resonance imaging (MRI), and Unified Parkinson Disease Rating Scale (UPDRS)[13] scoring by a movement disorders specialist (C.G.). Subjects were off antiparkinson medication for 18 hours prior to PET and UPDRS scoring. The local institutional review board approved the protocol; informed consent was obtained from all participants.

For PET imaging, subjects were pretreated with carbidopa, 2.5 mg/kg orally, and tolcapone (a COMT inhibitor), 200 mg, before the FDOPA scan. These pretreatment doses were given a mean of 59 minutes (range, 47–75 minutes; SD, 9 minutes) before the FDOPA scan and 65 minutes (range, 50–74 minutes; SD, 7 minutes) before the FMT scan. Because tolcapone has in rare cases been associated with liver damage,[14] serum AST, an index of liver function, was acquired at study enrollment and 2–4 weeks after the tolcapone dose. Potential subjects with abnormal baseline AST were excluded from the study.

FDOPA and FMT were synthesized by electrophilic fluorination of the appropriate stannylated precursors (for FMT, *N*-[trifluoroacetyl]-3-acetoxy-6-[trimethylstannyl]-l-phenylalanine ethyl ester; ABX, Radeberg, Germany) followed by flash chromatography

over alumina, hydrolysis in HBr, separation by semiprep HPLC, and a final workup to radiopharmaceutical purity.[15,16]

PET images were obtained on a Siemens ECAT EXACT HR+ PET scanner with an axial intrinsic resolution of 4.7 mm. Following intravenous injection of 5.2 mCi ± 10% of radiopharmaceutical, 18 three-dimensional dynamic frames were acquired over 90 minutes. The injected activity of FMT was within 5% of FDOPA injected activity (mean difference in injected doses was 0.6%). The mean interval between FMT and FDOPA PET scans was 35 days. During both the FDOPA and the FMT scans, urine was collected 95 and 185 minutes after injection.

MRI scans were obtained on a 3T SIGNA scanner using an 8-channel head coil, with higher-order shimming; a T1-weighted rapid gradient echo volume (MPRAGE; TR, 6.6 ms; TE, 2.8 ms; 166 1.2-mm axial slices) was used for coregistration to PET.

For image analysis, FDOPA and FMT PET sinograms were reconstructed by filtered back-projection into 18 volumes (time frames) of 128 × 128 × 63, 1.84 × 1.84 × 2.43 mm voxels, corrected for scatter, attenuation, and F-18 decay. Each frame was realigned within subject to the total sum image of the FDOPA study. The T1-weighted MRI was coregistered to the FDOPA sum image in native space, after which volumes of interest (VOIs), encompassing the caudate nucleus, putamen, and occipital cortex, were defined by single rater (C.G.) on the resampled MRI using in-house software (http://brainimaging.waisman.wisc.edu/~oakes/spam). The putamen was divided along its rostrocaudal axis into anterior, middle, and posterior segments of equal volume. An independent rater (J.H.), who was blind to the clinical status of the research subjects, used the time–activity curves from each volume to derive the normalized tissue uptake rate constant (K_{occ}).[17] K_{occ} values for each VOI were then sorted as ipsilateral or contralateral to the limb manifesting the initial motor symptoms. Bivariate (Pearson) correlations were computed between FMT and FDOPA K_{occ} values derived from 8 nonoverlapping subregions and between UPDRS III (motor) subscores and K_{occ} values from the contralateral whole putamen, in SPSS (version 16; Chicago, IL). For each tracer, K_{occ} values for subregions of the striatum were compared using paired-sample *t* tests. Because aging affects UPDRS scores[18] and possibly FDOPA uptake,[19] partial correlations with a covariate of age were also computed between UPDRS subscores and regional K_{occ} values.

Although more precise methods of calculating bladder wall radiation dose are available,[20] we made rough estimates of bladder wall exposure based on proportional activity in collected urine by comparison with a previous study of the effect of carbidopa pretreatment on FDOPA dosimetry.[21] The comparison study, which used similar void times, found that bladder wall exposure reached 68% of the estimated total exposure of 0.556 rad/mCi prior to the first void. To compare our data, we multiplied decay-corrected urine activity (in μCi/cc) by urine volume (cc) and then expressed this total bladder content activity as a proportion of injected dose. Bladder wall exposure from FMT was then estimated relative to published FDOPA values as (0.556 rad/mCi) × ([0.68][FMT/FDOPA proportion at void 1] + [0.32][FMT/FDOPA proportion at void 2]).

Results

1. A comparison of FDOPA to FMT uptake in 8 nonoverlapping regions (ipsilateral and contralateral caudate nucleus, anterior, middle, and posterior putamen) showed that K_{occ} values were correlated between the radiopharmaceuticals ($r = 0.8$; Fig. 1A), and that the difference between FMT and FDOPA K_{occ} values was greater for higher K_{occ} values (Fig. 1B).

2. In the presence of tolcapone pretreatment for FDOPA, the radiopharmaceuticals provided a similar range of K_{occ} values (FMT: range, 0.0184; mean, 0.013; SD, 0.005; FDOPA: range, 0.0172; mean, 0.0081; SD, 0.004). FMT displayed slightly better ability to distinguish the earlier from later-affected posterior putamen by the paired *t* test (*t*[df], *P*; −3.80[11], 0.003 for FMT and −3.25[11], 0.008 for FDOPA). Absolute differences in K_{occ} values between the posterior and anterior putamen, left and right putamen, and left and right posterior putamen were each greater for FMT than for FDOPA (paired *t* test, $P < .03$).

3. Within the striatum, the uptake profile differed in that FMT K_{occ} was maximal in the anterior putamen, whereas FDOPA K_{occ} was similar between the caudate nucleus and anterior putamen (Fig. 2). Mean caudate nucleus/whole putamen K_{occ} ratios (averaged between hemispheres) were 1.37 for FDOPA and 1.10 for FMT; mean anterior/posterior putamen ratios were 3.4 (SD, 2.5) for FDOPA and 2.3 (SD, 0.6) for FMT. The anterior/posterior putamen ratio differed significantly between brain hemispheres for FMT ($P = .015$) but less so for FDOPA ($P = .27$) because of the greater variance in the FDOPA ratio.

4. UPDRS III scores from the initially affected side of the body were inversely correlated with the contralateral putamen FMT K_{occ} ($r = −0.762$, $P < .005$) but not significantly with the FDOPA K_{occ} ($r = −0.512$, $P = .089$); scores for the later affected side of the body were also inversely correlated with the ipsilateral putamen FMT K_{occ} ($r = −.834$, $P = .001$) but less so with the FDOPA K_{occ} ($r = −0.552$, $P = .063$; Fig. 3). Partial correlations between UPDRS II and UPDRS III and striatal FMT uptake were significant; UPDRS II was also partially correlated with FDOPA uptake, but the magnitude of the correlation coefficients was less (Table 1).

5. Based on data from a pilot study conducted in 13 healthy individuals (mean age, 47 years) during which urine was collected from voids 2 and 3 hours postinjection, we found that FMT metabolites were excreted more rapidly into the urine than were FDOPA metabolites and that fractional excretion declined with age (Dejesus, unpublished). For these controls, the average fraction of administered radioactivity in the bladder at a mean of 107 and 186 minutes postinjection was 39% and 10%, respectively, for FMT, compared with 23% and 31%, respectively, for FDOPA.[21] In the PD subjects, mean fractional excretion at 95 and 185 minutes was 29.5% and 16%, respectively, for FMT and 24.5% and 12%, respectively, for FDOPA with tolcapone. Bladder wall exposure estimates comparing FMT/carbidopa with FDOPA/carbidopa[21] were 0.70 rad/mCi for controls and 0.58 rad/mCi for PD subjects.

6. No subjects showed a delayed elevation of AST after the single dose of tolcapone.

Discussion

To our knowledge, this is the first study in human subjects comparing FMT with FDOPA PET. We found that in early PD, the rostrocaudal gradient in uptake differed between the radiopharmaceuticals and that FMT was better correlated with clinical symptoms than FDOPA with incomplete COMT inhibition. Previous FDOPA studies of PD have shown that FDOPA uptake is best preserved in the anterior and ventral portions of the striatum, but is quantitatively similar between the caudate nucleus and anterior putamen.[22] In contrast, we found that FMT uptake in the anterior putamen exceeded that in the caudate nucleus. In young healthy individuals, no anterior–posterior gradient in striatal FDOPA uptake is detectable; with aging, slightly decreased uptake in the putamen relative to the rostral striatum, develops.[23]

The differing rostrocaudal uptake profile between FMT and FDOPA probably reflects biological differences in the trapped metabolites. FDOPA (an analogue of L-dopa) is taken up into catecholaminergic neurons, where it is decarboxylated by AAAD to fluorodopamine, which can be taken up into synaptic vesicles by vesicular monoamine transporter type 2 (VMAT2)[24] and cleared from the synaptic cleft by dopamine transporters (DATs).[25] COMT metabolizes both FDOPA and fluorodopamine to produce 3-*O*-methyl-flurodopa (3OMFD) and 3-*O*-methyl-p-tyramine, respectively.[26] 3OMFD crosses the blood–brain barrier, raising nonspecific background activity in FDOPA scans. Metabolism of fluorodopamine by the outer mitochondrial membrane enzyme monoamine oxidase type A (MAO-A) produces metabolic products 3,4-dihydroxyphenylacetic acid and then homovanillic acid (HVA) via COMT.[27]

FMT, in contrast, is not a substrate for COMT and has 10-fold greater affinity for AAAD than does FDOPA.[28] Its AAAD product amine, 6-fluoro-m-tyramine, has 1.5- to 3-fold greater affinity for the monoamine MAO-A than does fluorodopamine, with the resulting product fluoro-m-hydroxy-phenylacetic acid (FHPAA), which is trapped in the striatum.[27] FMT is a poor substrate for DATs and VMAT2 and so is not trapped in synaptic vesicles. Therefore, although FMT trapping reflects primarily AADC and MAO activity, FDOPA trapping also depends on COMT activity and on reuptake and vesicularization, making FDOPA useful for modeling dopamine turnover.[29] Thirty minutes after injection of rats with radiopharmaceutical, 28% of FDOPA has been metabolized by MAO-A and 30% by COMT, whereas 80%–90% of FMT had been metabolized to FHPAA by MAO-A.[27] Postmortem quantitative studies have shown dopamine concentrations in normal caudate nucleus to be 60%–103% that of putamen and concentrations of homovanillic acid (HVA) in the caudate nucleus to be 47%–76% of that in the putamen.[30] Therefore, the moderate difference we observed in rostrocaudal distribution between the radiopharmaceuticals probably reflects the degree to which production of their trapped products depends on MAO-A activity, the normal metabolic byproduct of which, HVA, is of a higher concentration in the putamen.

As a result of this gradient difference, ratios of caudate/ putamen and anterior/posterior putamen K_{occ} were lower for FMT, but may prove useful for distinguishing typical from atypical PD due to lower variance. Asselin found that FMT contralateral putamen K_{occ} for 21 Parkinsonian subjects was 50% of that for 3 normal subjects and that the caudate-to-putamen ratio was 1.6,[8] compared with 45% and 1.9, respectively, previously published for FDOPA.[31] The K_{occ} values and caudate nucleus/whole putamen ratios we computed differed slightly based on our VOI selection technique.[32]

We expected the higher signal-to-background ratio of FMT to improve our ability to measure disease-related alterations in specific uptake; within the striatum, FMT did produce more significant regional differences, but of a magnitude unlikely to be clinically useful. A within-subject comparison of FMT and FDOPA in a nonhuman primate model of PD concluded that the uptake rate constants were tightly correlated between radiopharmaceuticals and separated healthy from MPTP-lesioned striata equally well, but that variance in FMT K_{occ} values was greater, possibly because the fraction of FMT in plasma is very sensitive to the timing of carbidopa administration.[5] In comparison, we found that the standard deviation in K_{occ} values was similar when comparing FMT to FDOPA with COMT inhibition; this variance was similar in magnitude to that of FMT K_{occ} reported in the lesioned striata of nonhuman primates.[33] We suspect that inhibition of COMT by tolcapone shifted the biochemical properties of FDOPA toward that of a “pure” AAAD agonist (similar to FMT), increasing the mean and range of its K_{occ} values. During FDOPA scans, pretreatment with COMT inhibitors produces marked increases in uptake measures that rely on a tissue reference region, such as K_{occ} and striatal-occipital ratios, in contrast

with those generated using a metabolite-corrected plasma input such as K_i.[34] In a model that assumes irreversible trapping, this uptake rate constant is a ratio of the quantity of tracer ultimately trapped in the striatum relative to its availability (in blood or reference tissue) over time. During FDOPA studies, radioactivity in the reference tissue overestimates the quantity of tracer available for trapping because a portion of the activity is "untrappable" 3OMFD. This metabolite therefore reduces the magnitude of K_{occ} values calculated using a tissue reference.

The primary question raised by this study is why FMT trapping, which follows the physiological pathway of dopamine metabolism less faithfully than FDOPA, better reflected clinical symptoms. Figures 1 and 3 suggest that correlation values were improved by the ability of FMT to spread high K_{occ} values. A number of cross-sectional studies have shown significant correlation between FDOPA uptake and clinical symptoms. Akinesia and rigidity are correlated with lower FDOPA uptake, whereas more severe tremor is associated with preserved uptake in the caudate nucleus relative to the putamen.[31] In 35 PD subjects off medication, striatal FDOPA K_{occ} was correlated with bradykinesia ($r = -0.64$) and rigidity ($r = -0.59$).[35] Using [^{123}I]CIT, a dopamine transporter ligand, the correlation of striatal binding with UPDRS II scores was −0.68 and with UPDRS III scores was −0.56.[2] Because the magnitude of these correlations is similar to those we found between putamen FDOPA K_{occ} and UPDRS III, the lack of significance of other FDOPA correlations in the present study may simply reflect inadequate statistical power.

Correlations between parkinsonian symptoms and striatal FMT uptake have been investigated in nonhuman primate models. In 14 monkeys lesioned unilaterally with MPTP, the degree of asymmetry in putamen K_{occ} values correlated with the degree of limb tremor asymmetry.[36] A human study of persons with movement disorders related the pattern of FMT uptake to the clinical subtype, but did not specifically correlate this with clinical scores.[8] Recently, putamenal infusions of adeno-associated viral type 2 vectors containing the human *AADC* gene in 10 PD subjects resulted in a dose-dependent increase in FMT uptake and improved UPDRS scores.[37] In nonhuman primates, similar infusions produced improvement in striatal FMT uptake and clinical scores. Histology confirmed transduction of striatal neurons with medium spiny morphology.[38] Our results also suggest that residual AAAD activity is a major determinant of functional status.

The results of this study suggest that FMT performs well as a biomarker for clinical symptoms in PD. A larger prospective study of PD subjects and normal controls should be done to evaluate the diagnostic sensitivity of FMT and to what degree it reflects clinical changes longitudinally. The urine and AST measurements add information that improves the risk/benefit ratio for using 5-mCi doses of FMT and single 200-mg doses of tolcapone as pretreatment for FDOPA studies in human subjects. Four subjects in this study were being treated with MAO-B inhibitors, which were held for 24 hours prior to PET scanning, but a residual effect of MAO inhibition on FMT uptake cannot be excluded, as the duration of washout is probably weeks.[39] Measurements of FDOPA metabolites to quantify the effect of 200 mg of tolcapone are also needed.

Acknowledgments

Funding agencies: This work was supported by the Department of Veterans Affairs, Veterans Health Administration, Office of Research and Development, Clinical Science Research and Development Service and University of Wisconsin Institute for Clinical and Translational Research, funded through a National Institutes of Health Clinical and Translational Science Award (grant number 1UL1RR025011). This work was supported with the use of facilities at the William S. Middleton Memorial Veterans Hospital Geriatric Research Education and Clinical Center and the Waisman Laboratory for Brain Imaging and Behavior, Madison, Wisconsin.

References

1. Whone AL, Watts RL, Stoessl AJ, et al. Slower progression of Parkinson's disease with ropinirole versus levodopa: the REAL-PET study. Ann Neurol. 2003; 54:93–101. [PubMed: 12838524]
2. Pirker W. Correlation of dopamine transporter imaging with parkinsonian motor handicap: how close is it? Mov Disord. 2003; 18 Suppl 7:S43–S51. [PubMed: 14531046]
3. Morrish PK, Sawle GV, Brooks DJ. An [18F]dopa-PET and clinical study of the rate of progression in Parkinson's disease. Brain. 1996; 119:585–591. [PubMed: 8800950]
4. Sossi V, Doudet DJ, Holden JE. A reversible tracer analysis approach to the study of effective dopamine turnover. J Cereb Blood Flow Metab. 2001; 21:469–476. [PubMed: 11323532]
5. Doudet DJ, Chan GL, Jivan S, et al. Evaluation of dopaminergic presynaptic integrity: 6-[18F]fluoro-L-dopa versus 6-[18F]fluoro-L-m-tyrosine. J Cereb Blood Flow Metab. 1999; 19:278–287. [PubMed: 10078880]
6. DeJesus OT, Holden JE, Endres C, et al. Visualization of dopamine nerve terminals by positron tomography using [18F]fluoro-beta-fluoromethylene-m-tyrosine. Brain Res. 1992; 597:151–154. [PubMed: 1477728]
7. Firnau, G.; Chirakal, R.; Wahl, L., et al. New PET tracers for cerebral dopamine: should 6-[18F]Fluoro-l-dopa be replaced. In: Emran, AM., editor. Chemists Views of Imaging Centers. New York: Plenum Press; 1995. p. 237-247.
8. Asselin, R. Brain Imaging Using PET. San Diego, CA: Academic Press; 2002. Patterns of distribution of [18F]-6-Fluoro-L-m-tyrosine in PET images of patients with movement disorders.
9. Mamo D, Remington G, Nobrega J, et al. Effect of acute antipsychotic administration on dopamine synthesis in rodents and human subjects using 6-[F-18]-L-m-tyrosine. Synapse. 2004; 52:153–162. [PubMed: 15034921]
10. Eberling JL, Jagust WJ, Christine CW, et al. Results from a phase I safety trial of hAADC gene therapy for Parkinson disease. Neurology. 2008; 70:1980–1983. [PubMed: 18401019]
11. Wilcox CE, Braskie MN, Kluth JT, Jagust WJ. Overeating behavior and striatal dopamine with 6-[F]-Fluoro-L-m-Tyrosine PET. J Obes. 2010 [Epub ahead of print].
12. Gibb WR, Lees AJ. The relevance of the Lewy body to the pathogenesis of idiopathic Parkinson's disease. J Neurol Neurosurg Psychiatry. 1988; 51:745–752. [PubMed: 2841426]
13. Fahn, S.; Elton, RL.; Members, UP. Unified Parkinson's Disease Rating Scale. In: Fahn, S.; Marsden, CD.; Goldstein, M.; Calne, DB., editors. Recent Developments in Parkinson's Disease. Florham Park, NJ: McMillan Healthcare Information; 1987. p. 153-163.p. 293-304.
14. Keating GM, Lyseng-Williamson KA. Tolcapone: a review of its use in the management of Parkinson's disease. CNS Drugs. 2005; 19:165–184. [PubMed: 15697329]
15. Nickles R, Daube M, Ruth T. An oxygen-18 gas target for the production of [F-18] F2. Int J Appl Rad Isotopes. 1984; 35:117–123.
16. Namavari M, Satyamurthy N, Phelps ME, Barrio JR. Synthesis of 6-[18F] and 4-[18F]fluoro-L-m-tyrosines via regioselective radio-fluorodestannylation. Appl Radiat Isot. 1993; 44:527–536. [PubMed: 8472025]
17. Patlak CS, Blasberg RG. Graphical evaluation of blood-to-brain transfer constants from multiple-time uptake data. Generalizations. J Cereb Blood Flow Metab. 1985; 5:584–590. [PubMed: 4055928]
18. Levy G, Louis ED, Cote L, et al. Contribution of aging to the severity of different motor signs in Parkinson disease. Arch Neurol. 2005; 62:467–472. [PubMed: 15767513]
19. Nurmi E, Ruottinen HM, Bergman J, et al. Rate of progression in Parkinson's disease: a 6-[18F]fluoro-L-dopa PET study. Mov Disord. 2001; 16:608–615. [PubMed: 11481683]
20. Thomas SR, Stabin MG, Chen CT, Samaratunga RC. MIRD Pamphlet No. 14 revised: A dynamic urinary bladder model for radiation dose calculations. Task Group of the MIRD Committee, Society of Nuclear Medicine. J Nucl Med. 1999; 40:102S–123S. [PubMed: 10210232]
21. Brown WD, Oakes TR, DeJesus OT, et al. Fluorine-18-fluoro-L-DOPA dosimetry with carbidopa pretreatment. J Nucl Med. 1998; 39:1884–1891. [PubMed: 9829576]

22. Bruck A, Aalto S, Nurmi E, Vahlberg T, Bergman J, Rinne JO. Striatal subregional 6-[18F]fluoro-L-dopa uptake in early Parkinson's disease: a two-year follow-up study. Mov Disord. 2006; 21:958–963. [PubMed: 16550545]
23. Garnett ES, Lang AE, Chirakal R, Firnau G, Nahmias C. A rostrocaudal gradient for aromatic acid decarboxylase in the human striatum. Can J Neurol Sci. 1987; 14(3 Suppl):444–447. [PubMed: 3119181]
24. Erickson JD, Eiden LE, Hoffman BJ. Expression cloning of a reserpine-sensitive vesicular monoamine transporter. Proc Natl Acad Sci U S A. 1992; 89:10993–10997. [PubMed: 1438304]
25. Endres CJ, Swaminathan S, DeJesus OT, et al. Affinities of dopamine analogs for monoamine granular and plasma membrane transporters: implications for PET dopamine studies. Life Sci. 1997; 60:2399–2406. [PubMed: 9199484]
26. Firnau G, Sood S, Chirakal R, Nahmias C, Garnett ES. Metabolites of 6-[18F]fluoro-L-dopa in human blood. J Nucl Med. 1988; 29:363–369. [PubMed: 3126278]
27. DeJesus OT. Positron-labeled DOPA analogs to image dopamine terminals. Drug Dev Res. 2003; 59:249–260.
28. Dejesus OT, Murali D, Nickles RJ. Synthesis of brominated and fluorinated ortho-tyrosine analogs as potential DOPA decarboxylase tracers. J Label Comp Radiopharm. 1995; 37:147–149.
29. Sossi V, de La Fuente-Fernandez R, Holden JE, et al. Increase in dopamine turnover occurs early in Parkinson's disease: evidence from a new modeling approach to PET 18 F-fluorodopa data. J Cereb Blood Flow Metab. 2002; 22:232–239. [PubMed: 11823721]
30. Adolfsson R, Gottfries CG, Roos BE, Winblad B. Post-mortem distribution of dopamine and homovanillic acid in human brain, variations related to age, a review of the literature. J Neural Transm. 1979; 45:81–105. [PubMed: 381583]
31. Brooks DJ, Ibanez V, Sawle GV, et al. Differing patterns of striatal 18F-dopa uptake in Parkinson's disease, multiple system atrophy, and progressive supranuclear palsy. Ann Neurol. 1990; 28:547–555. [PubMed: 2132742]
32. Braskie MN, Wilcox CE, Landau SM, et al. Relationship of striatal dopamine synthesis capacity to age and cognition. J Neurosci. 2008; 28:14320–14328. [PubMed: 19109513]
33. Doudet DJ, Chan GLY, Jivan S, et al. Evaluation of dopaminergic presynaptic integrity 6-[F-18]fluoro-L-dopa versus 6-[F-18]fluoro-L-m-tyrosine. J Cereb Blood Flow Metab. 1999; 19:278–287. [PubMed: 10078880]
34. Sawle GV, Burn DJ, Morrish PK, et al. The effect of entacapone (OR-611) on brain [18F]-6-L-fluorodopa metabolism: implications for levodopa therapy of Parkinson's disease. Neurology. 1994; 44:1292–1297. [PubMed: 8035933]
35. Vingerhoets FJ, Schulzer M, Calne DB, Snow BJ. Which clinical sign of Parkinson's disease best reflects the nigrostriatal lesion? Ann Neurol. 1997; 41:58–64. [PubMed: 9005866]
36. Eberling JL, Pivirotto P, Bringas J, Bankiewicz KS. Tremor is associated with PET measures of nigrostriatal dopamine function in MPTP-lesioned monkeys. Exp Neurol. 2000; 165:342–346. [PubMed: 10993693]
37. Christine CW, Starr PA, Larson PS, et al. Safety and tolerability of putaminal AADC gene therapy for Parkinson disease. Neurology. 2009; 73:1662–1669. [PubMed: 19828868]
38. Bankiewicz KS, Forsayeth J, Eberling JL, et al. Long-term clinical improvement in MPTP-lesioned primates after gene therapy with AAV-hAADC. Mol Ther. 2006; 14:564–570. [PubMed: 16829205]
39. Palhagen S, Heinonen EH, Hagglund J, et al. Selegiline delays the onset of disability in de novo parkinsonian patients. Swedish Parkinson Study Group. Neurology. 1998; 51:520–525. [PubMed: 9710028]

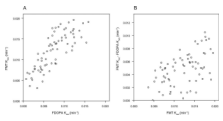

FIG. 1.

A: FMT K_{occ} was plotted against FDOPA K_{occ} for 8 nonoverlapping striatal subregions, yielding a linear (Pearson) correlation coefficient of 0.8. **B:** FMT K_{occ} was plotted against the difference between FMT K_{occ} and FDOPA K_{occ} for the same subregions.

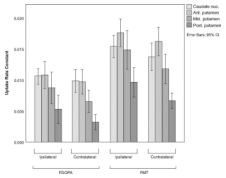

FIG. 2.

Uptake rate constants (K_{occ}) for 8 striatal subregions ipsilateral and contralateral to initial symptoms for FDOPA (left) and FMT (right). Error bars represent 95% confidence intervals; nuc., nucleus; Ant., anterior; Mid., middle; Post., posterior.

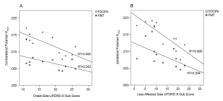

FIG. 3.

UPDRS III (motor) subscores from the initially affected (**A**) and later affected (**B**) sides of the body versus whole putamen K_{occ} from the opposite brain hemisphere, plotted separately for FMT (triangles) and FDOPA (circles).

TABLE 1

Partial correlations between FMT and FDOPA K_{occ} and UPDRS subscores

Clinical measure	Brain hemisphere	Structure	FDOPA	FMT
UPDRS II	CL	Caudate nucleus	−0.685[a]	−0.812[a]
		Whole putamen	−0.702[a]	−0.819[a]
		Posterior putamen	−0.498	−0.723[a]
	IL	Caudate nucleus	−0.442	−0.686[a]
		Putamen	−0.741[a]	−0.875[a]
		Posterior putamen	−0.615	−0.887[a]
UPDRS III	CL	Caudate nucleus	−0.239	−0.524
	IL	Putamen	−0.437	−0.727[a]
		Posterior putamen	−0.213	−0.591
UPDRS III	IL	Caudate nucleus	−0.148	−0.645[a]
	CL	Putamen	−0.455	−0.794[a]
		Posterior putamen	−0.235	−0.647[a]

CL, contralateral to initial motor symptoms; FDOPA, [^{18}F]fluoro-L-dopa; FMT, 6-[^{18}F]fluoro-m-tyrosine; IL, ipsilateral to initial motor symptoms.

[a]Partial correlation coefficients (controlled for age) > 0.6 are significant (2-tailed *t* statistic, $P < .05$).